Journal of Inflammation Research

Dovepress
Taylor & Francis Group

Open Access Full Text Article

ORIGINAL RESEARCH

Causal Association Between Genetically Predicted Circulating Metabolites and Pressure Ulcers: A Two-Sample Mendelian Randomization Study

Xiaoli Hu[1], Yue Zhang[2], Yuchao Wu[3], Miao Peng[4]

[1]Department of Gastroenterology, The Affiliated Hospital of Southwest Medical University, Luzhou, People's Republic of China; [2]Department of Pain Management, The Affiliated Hospital of Southwest Medical University, Luzhou, People's Republic of China; [3]Emergency Intensive Care Unit, The Affiliated Hospital of Southwest Medical University, Luzhou, People's Republic of China; [4]Department of Critical Care Medicine, The Affiliated Hospital of Southwest Medical University, Luzhou, People's Republic of China

Correspondence: Miao Peng, Department of Critical Care Medicine, The Affiliated Hospital of Southwest Medical University, 25 Taiping Street, Jiangyang District, Luzhou, Sichuan, 646000, People's Republic of China, Tel +86-15181977618, Email threewaterpm@swmu.edu.cn

Introduction: Pressure ulcers (PU) are skin and soft tissue injuries caused by prolonged localized pressure, friction, or shear forces, particularly affecting individuals with limited mobility. Understanding the mechanisms behind PU formation, including the role of metabolites, is crucial for effective prevention.

Methods: We conducted a two-sample MR analysis to explore the causal relationship between circulating metabolites and PU. Exposure data included GWAS data for 1400 metabolites, while outcome data were sourced from a Finnish database. We used multiple MR methods (IVW, MR-Egger, WM, Simple mode, Weighted mode) to estimate causal effects and performed sensitivity analyses to assess robustness. Additionally, we validated the effects of key metabolites on PU through animal experiments.

Results: A total of 19 metabolites demonstrated significant causal associations with PU ($P < 0.01$). Among them, 7 metabolites were linked to PU increased risk, the highest ORs was (IVW: OR [95% CI] = 1.3690 [1.0852–1.7270]; P = 0.0080) for the spermidine to choline ratio. 12 metabolites with positive effects on PU prevention, the homostachydrine levels showing a highest association (IVW: OR [95% CI] = 0.7497 [0.6206–0.9056]; P = 0.0028). Sensitivity analyses supported these findings and validated the stability of the results. In animal experiments, rats treated with HD-Hom and LR (Spe/Cho) showed the fastest scab shedding and new epithelial tissue formation, with the smallest residual wound area.

Conclusion: This study highlights significant causal relationships between circulating metabolites and PU risk. The identification of the spermidine to choline ratio as a risk factor and homostachydrine levels as a protective factor suggests potential metabolic targets for PU prevention and treatment.

Keywords: pressure ulcers, metabolites, Mendelian randomization, causal relationship, circulating metabolites

Introduction

Pressure ulcer (PU), also known as a pressure injury, are a type of skin and soft tissue injury caused by persistent localized pressure, friction, or shear forces.[1–3] The condition occurs mainly on bony prominences of the body, such as the sacrum, hips and heels, and is common in patients who are bedridden or have limited mobility, especially in the elderly population.[4] Globally, the incidence of PU can be as high as 15–30% in hospitalized patients and 30–50% in long-term care facilities.[5,6] As the global trend of aging increases, the incidence of PUs continues to rise, placing a heavy burden on patients and their caregivers.[7]

Pressure ulcer is a multifactorial and complex disease, and its mechanism involves various aspects such as mechanical pressure, moist environment, malnutrition and underlying diseases.[8,9] Although the traditional view is that ischemic injury caused by external forces is the main cause of pressure ulcer formation, this mechanism cannot fully explain all cases of PU.[10] In recent years, researchers have gradually turned their attention to exploring other possible mechanisms,

Received: 19 November 2024
Accepted: 16 May 2025
Published: 28 May 2025

including: reperfusion injury after ischemia, abnormal collagen synthesis, impaired lymphatic return, altered tissue fluid flow, and persistent cellular deformation.[11,12] Sustained pressure not only directly affects local tissues, but may also lead to changes in circulating metabolite profiles.[13,14]

Metabolites play a key role in the maintenance of human health, especially in physiological processes such as tissue repair, inflammatory response and immune response.[15–17] Circulating metabolites not only serve as energy sources, but also as signaling molecules that regulate the physiological state and function of cells. In the case of PU, studies have shown that changes in the levels of certain metabolites are closely related to the intensity of the inflammatory response as well as the efficiency of tissue repair. For example, Phytanate was found to be potentially linked to tissue inflammatory responses and oxidative stress, with abnormal levels possibly affecting local tissue metabolism and healing processes.[18] Understanding the role of metabolites in the development and healing of PU may provide new ideas for clinical intervention and facilitate the development of effective treatment strategies. By examining metabolite levels, researchers can discern variations in normal and pathological states.[19] This approach can improve our understanding, diagnosis, and management of PU. However, research specifically focusing on the application of metabolomics to PU is still limited, highlighting a significant need for further study.

Mendelian randomization (MR) is a robust approach for causal inference that uses genetic variants as instrumental variables (IVs), effectively eliminating the confounding bias present in traditional epidemiological studies.[20–25] Through genomic association studies (GWAS), researchers can identify genetic variants associated with specific phenotypes or diseases, and thus assess the causal impact of these variants on health outcomes without bias.[26–28] This approach not only improves the reliability of study results, but also provides a powerful tool for a deeper understanding of the causal relationship between metabolites and PU.[29]

Given the high prevalence of PU and their serious implications, it has become particularly important to gain a deeper understanding of their mechanisms and potential biomarkers. The aim of this study was to investigate the causal association between genetically predicted circulating metabolites and PU by a two-sample MR method.

Materials and Methods

Study Design

This study utilized a two-sample MR approach to investigate the causal relationship between 1400 circulating metabolites and PU. To ensure the validity of instrumental variables (IVs) in causal inference, this study fulfils the following three key assumptions: (1) The genetic variants, specifically single nucleotide polymorphisms (SNPs), must be strongly associated with the exposure, which in this study refers to "circulating metabolites"; (2) The SNPs should not be related to any potential confounders between the exposure and the outcome, which in this case is "pressure ulcers"; and (3) The SNPs must influence the outcome solely through their effect on the exposure. Figure 1 illustrates the overall analysis workflow.

GWAS Data Sources for Circulating Metabolites

The exposure data comprised genome-wide association study (GWAS) data for 1400 circulating metabolites, including 1091 metabolite levels and 309 metabolite ratios. These data were obtained from the GWAS Catalog (https://www.ebi.ac.uk/gwas/studies/GCST90199621-90201020). The study population consisted exclusively of individuals of European ancestry, in order to minimize potential confounding related to genetic ancestry. A detailed overview of the GWAS data sources used for the exposure factors in this study is provided in Table S1.

GWAS Data Sources for PU

The GWAS data for PU were obtained from the Finnish database (https://www.finngen.fi/en), with the specific download link available at https://storage.googleapis.com/finngen-public-data-r11/summary_stats/finngen_R11_L12_DECUBITANSULCERANDPRESSURE.gz. This GWAS analysis was conducted on 424,909 individuals of European ancestry, including 1868 cases and 423,041 controls. Following quality control procedures, a total of 21,306,340 SNPs were analyzed. This study was

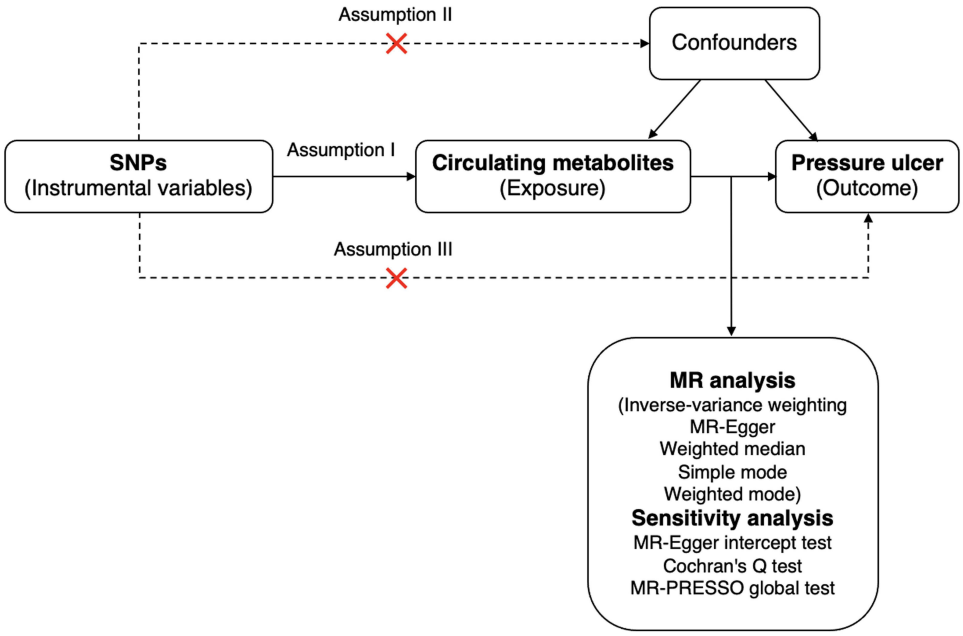

Figure 1 Overview of the Mendelian Randomization study.

approved by the Ethics Committee of the Affiliated Hospital of Southwest Medical University. The research was conducted in accordance with the ethical standards outlined in the Declaration of Helsinki and relevant national guidelines.

Selection of IVs

First, SNPs loci associated with PU were screened using a significance threshold of $P < 5\times10^{-6}$ to test the hypothesis. Second, linkage disequilibrium (LD) adjustment parameters ($r^2 = 0.001$ and kilobase (kb) = 10,000) were used to eliminate LD correlations, and SNPs with $r^2 > 0.001$ and kb < 10,000 were excluded from the analysis to fulfill the hypothesis. Finally, heterogeneous SNPs with F-statistic values < 10 were excluded from further analysis, while eligible SNPs were retained as valid IVs to fulfill the hypothesis. This systematic approach aims to establish robust causal relationships between circulating metabolites and PU using MR analysis, ensuring rigorous selection and validation of IVs.

Model Construction and Treatment

All animal experimental designs were strictly conducted in accordance with the Sichuan Province Laboratory Animal Management Measures and were approved by the Ethics Committee of Southwest Medical University (Approval No.: 20240813-002). A total of thirty-six male SD rats (8 weeks old, SPF grade) were purchased from Beijing Vital River Laboratory Animal Technology Co., Ltd. (Beijing, China). The animals were acclimated for one week in a controlled environment with a temperature of 23±1°C and a constant humidity of 60±10%, with free access to standard food and water, and a 12-hour light/12-hour dark cycle. Subsequently, a pressure ulcer rat model was established.[30,31] After modeling, the rats were divided into two groups: the oral gavage group and the intraperitoneal injection group.

The oral gavage group was divided into three subgroups (six rats of each group): (1) Model group (administered the same volume of 0.9% NaCl after modeling, continuous gavage for 7 days); (2) LD-Hom group (treated with low-dose Homostachydrine after modeling, administered Homostachydrine at 10 mg/kg.d, continuous gavage for 7 days); (3) HD-Hom group (treated with high-dose Homostachydrine after modeling, administered Homostachydrine at 30 mg/kg·d, continuous gavage for 7 days).

The intraperitoneal injection group was divided into three subgroups (six rats of each group): (1) Model group (administered the same volume of 0.9% NaCl after modeling, continuous intraperitoneal injection for 7 days); (2) LR (Spe/Cho) group (intraperitoneally injected with low ratio Spermidine: Choline (50:50 mg/kg·d) after modeling, continuous injection for 7 days); (3) HR (Spe/Cho) group (intraperitoneally injected with high ratio Spermidine: Choline

https://doi.org/10.2147/JIR.S503370

(50:10 mg/kg·d) after modeling, continuous injection for 7 days). The pressure ulcer conditions of the rats in different groups were observed at 1, 3, and 7 days after modeling. All animals were used in accordance with the approved protocol by the Institutional Animal Care and Use.

Wound Healing Observation

The wounds were observed routinely every day after treatment, and photographs of the wounds were taken on days 1, 3, and 7 after treatment. A ruler with a minimum scale of 1 mm was placed at the edge of the wound, and the camera lens was kept parallel to the wound. The wound area was calculated using ImageJ software (Wound area = Long axis radius × Short axis radius × π). Wound healing was considered complete when the wound was fully covered by epithelial tissue or new skin. The wound healing rate was calculated as follows: Wound healing rate (%) = (Initial wound area - Measured wound area on the day) / Initial wound area × 100%.

Hematoxylin and Eosin (HE) Staining

On day 7 after treatment, the rats were euthanized by intraperitoneal anesthesia. A square piece of skin (15 mm^2) centered on the wound was excised. The skin sample was fixed in 4% paraformaldehyde solution at room temperature for 48 hours, followed by dehydration, paraffin embedding, and sectioning. The structural characteristics of the wound skin, the formation of granulation tissue, and the infiltration of inflammatory cells were observed using HE staining. The steps consisted of removing paraffin, rehydrating the sections, and applying hematoxylin for 5 minutes (Beyotime Biotechnology, China). The sections were then treated with 1% acid alcohol for differentiation, exposed to ammonia water for bluing, and stained with eosin Y (Sigma-Aldrich, St. Louis, MO, USA) for 2 minutes as a counterstain. After dehydration and clearing, the sections were mounted for examination.

Masson Staining

On day 7 post-treatment, the rats were euthanized via intraperitoneal anesthesia. A 15 mm^2 skin sample centered on the wound was collected and fixed in 4% paraformaldehyde for 48 hours. Subsequently, the sample was dehydrated, paraffin - embedded, and sectioned. Masson staining was performed. The sections were first treated with Bouin's solution and then sequentially stained with Biebrich scarlet-acid fuchsin, phosphotungstic/phosphomolybdic acid, and aniline blue, following the protocol provided by Sigma-Aldrich. Through these steps, the deposition and arrangement of collagen fibers in the wound were observed.

Western Blot

Proteins expression in rat skin tissue from the wound area of the in vivo model were analyzed by Western blot. The BCA protein concentration assay kit was used for protein quantification. Equal amounts of protein were separated using 10% sodium dodecyl sulfate-polyacrylamide gel electrophoresis (SDS-PAGE) and transferred from the gel to nitrocellulose membrane, blocked for 1 h with 5% skimmed milk in Tris-buffered saline containing 0.1% Tween-20 at room temperature. The membranes were incubated overnight at 4°C with the primary antibodies: anti-TNF-α (1:1000, ab183218, Abcam), anti-COL-I (1:1000, ab138492, Abcam), anti-COL-III (1:1000, ab184993, Abcam), and anti-GAPDH (1:1000, ab8245, Abcam). The membranes were washed three times with PBS and incubated with HRP-conjugated goat anti-rabbit IgG secondary antibodies (1:2000, ab205719, Abcam) for 90 min at room temperature. Protein bands were visualized using the ECL chemiluminescence substrate kit (Beijing labgic Biotechnology CO., LTD. Beijing, China) according to the manufacturer's protocol and analyzed using Image J software (version 1.8; National Institutes of Health). GAPDH was used as the loading control.

Statistical Analysis

MR analysis was conducted using five different methods: inverse-variance weighting (IVW), MR-Egger, weighted median (WM), simple mode, and weighted mode. The IVW method was the primary approach for estimating causal effects, with the significance level set at $P < 0.01$. Heterogeneity among the instrumental variables (IVs) affecting PU was assessed using MR-Egger regression and Cochran's Q test. If significant heterogeneity was detected ($P < 0.05$),

a random-effects IVW model was used for causal inference. In contrast, if no significant heterogeneity was found ($P \geq 0.05$), a fixed-effects IVW model was applied. This comprehensive approach ensured a rigorous evaluation of the relationships by combining various MR techniques to enhance the reliability and validity of the results.

Sensitivity analyses included MR-Egger regression and the MR-PRESSO method to assess horizontal pleiotropy, which evaluates whether the IVs influence the outcome through pathways other than the exposure of interest. A regression intercept P-value > 0.05 indicated no evidence of such pleiotropy. The "leave-one-out" analysis was performed to examine the influence of individual SNPs on the causal relationship: each SNP was sequentially removed, and the combined effect estimate of the remaining SNPs was recalculated to assess the impact of each SNP on the overall MR analysis results. These sensitivity analyses aimed to ensure the robustness of the MR findings by detecting and addressing potential biases, such as horizontal pleiotropy and the effects of individual SNPs.

The analyses were conducted using RStudio version 2024.04.0+735, with the following packages: "TwoSampleMR", "ieugwasr", "VariantAnnotation", and "gwasglue2".

Results

Causal Relationship Between Circulating Metabolites and PU

A comprehensive MR analysis was conducted to explore the causal effects of 1400 circulating metabolites on PU. The primary approach employed was the IVW method, with stringent control for linkage disequilibrium (LD) and potential confounding factors, aiming to identify metabolites that play a significant role in the development and progression of PU. Figure 2 illustrates the causal associations between circulating metabolites and PU, showing those with at least one MR analysis method reaching a significance level of $P < 0.05$. Table 1 presents a list of 77 circulating metabolites that exhibited potential causal relationships with PU based on the IVW method at a significance level of $P < 0.05$.

Causal Relationships Between 19 Significantly Associated Circulating Metabolites and PU

We identified metabolites that exhibited consistent odds ratio (OR) directions across all five MR methods and achieved a significance threshold of $P < 0.01$ in the IVW method. Ultimately, 19 plasma metabolites were found to be significantly associated with PU, as detailed in Table 2 and Figure 3. Among these, seven metabolites were closely linked to an increased risk of PU, with the highest OR observed for the spermidine to choline ratio (IVW: OR [95% CI] = 1.3690 [1.0852–1.7270]; P = 0.0080). Conversely, 12 metabolites demonstrated a protective effect against PU, with the lowest OR observed for homostachydrine levels (IVW: OR [95% CI] = 0.7497 [0.6206–0.9056]; P = 0.0028).

Further Investigation of the Causal Effects of Spermidine to Choline Ratio and Homostachydrine Levels on PU

Among the 19 significantly associated circulating metabolites, the spermidine to choline ratio (IVW: OR [95% CI] = 1.3690 [1.0852–1.7270]; P = 0.0080) and homostachydrine levels (IVW: OR [95% CI] = 0.7497 [0.6206–0.9056]; P = 0.0028) were identified as the factors with the most substantial influence on reducing and increasing PU risk, respectively. This finding prompted us to conduct a more in-depth analysis of these two relationships.

Our analysis included the examination of 17 and 24 SNPs using the IVW method, respectively, ultimately confirming a significant causal relationship between the spermidine to choline ratio and homostachydrine levels with PU (see Figures 4A, B, 5A and B). Furthermore, our study found no evidence of heterogeneity or horizontal pleiotropy, reinforcing the validity of our results (Table 3). The MR-Egger regression analysis, illustrated in Figures 4C and 5C, showed minimal intercepts and low I^2 statistics, indicating that there was no significant horizontal pleiotropy affecting the MR analysis.

The results of the leave-one-out sensitivity analysis, presented in Figures 4D and 5D, demonstrated that the removal of individual SNPs did not significantly impact the overall causal relationship assessment. This suggests that the association between the spermidine to choline ratio and homostachydrine levels with PU is not influenced by any single genetic variant acting as an instrumental variable. These analytical results affirm the accuracy and robustness of our study conclusions.

 https://doi.org/10.2147/JIR.S503370

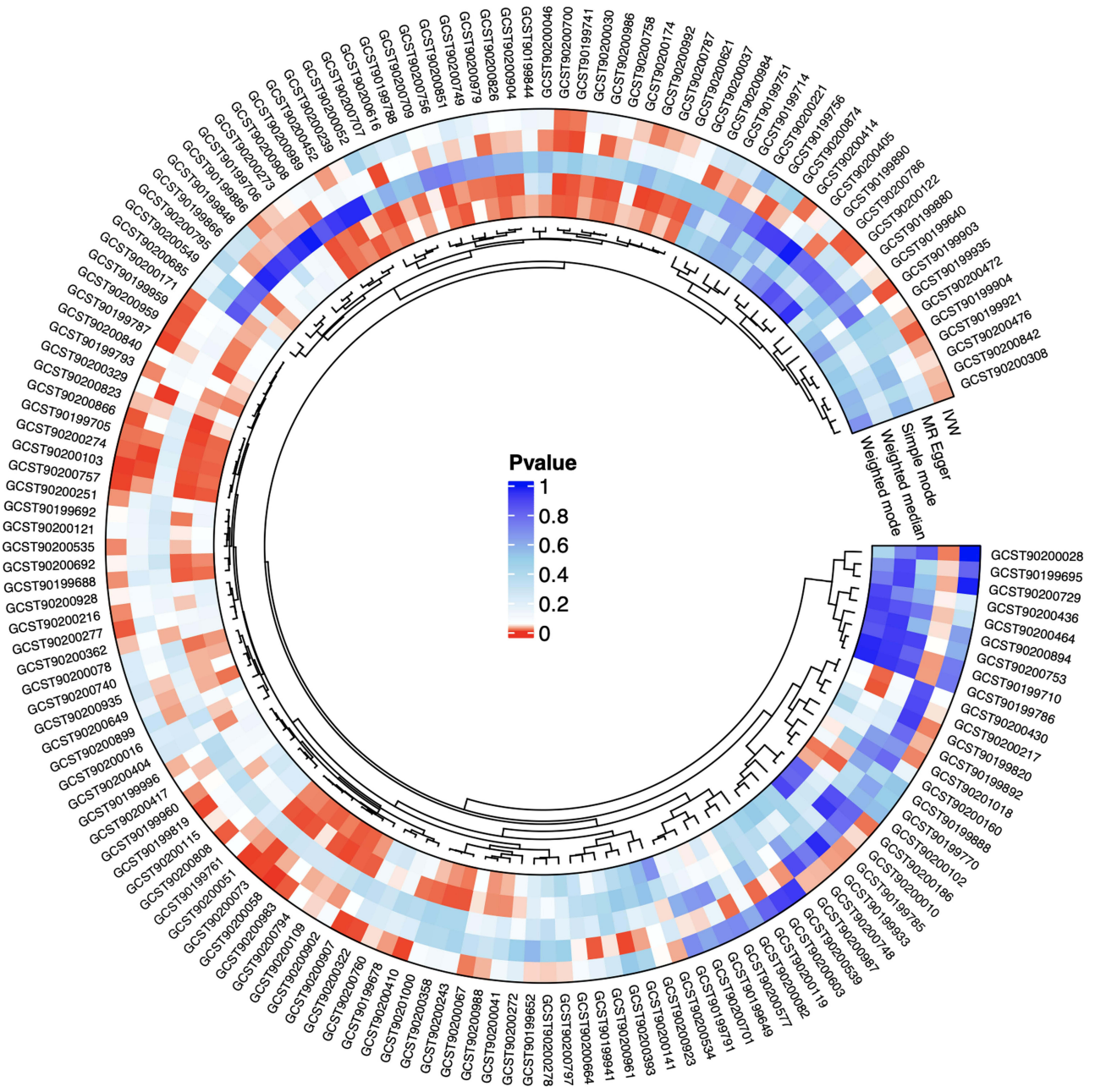

Figure 2 Circular plot of MR Analysis. The outer ring displays the metabolite IDs, the inner ring represents different MR methods. Each small square indicates the p-value from the MR analysis. Red color denotes p-values less than 0.05, with deeper shades indicating smaller p-values.

Homostachydrine and HR (Spe/Cho) Promote the Healing of Pressure Ulcer Wounds

Next, a pressure ulcer rat model was established and treated with different doses of Homostachydrine and Spermidine/choline. Wound healing was observed on days 1, 3, and 7 post-treatment, as shown in Figure 6. On day 1, no significant differences were observed among the groups. By day 3, the model group exhibited partial inflammatory exudation and incomplete scab coverage, while the LR (Spe/Cho) group showed a similar condition to the model group, with no significant improvement. In contrast, the LD-Hom group demonstrated significantly better outcomes than the model group, with dry wounds, no exudation, thin scab formation, and improved healing ($P<0.05$). The HD-Hom and HR (Spe/Cho) groups showed even greater efficacy, with dry wounds and a clear trend toward healing ($P<0.001$). By day 7, the wounds in the model and LR (Spe/Cho) groups were still covered

Table 1 The Causal Relationship Between 77 Circulating Metabolites and Pressure Ulcer Demonstrated by IVW Method for MR Analysis

ID.exposure	Exposure	Nsnp	p-value	OR	OR_lci95	OR_uci95
GCST90200058	1-(1-enyl-stearoyl)-2-arachidonoyl-GPE (p-18:0/20:4) levels	24	0.0005	1.3008	1.1228	1.5071
GCST90200103	Linoleoyl-arachidonoyl-glycerol (18:2/20:4) [1] levels	20	0.0016	1.1791	1.0646	1.3058
GCST90200051	1-palmitoyl-2-dihomo-linolenoyl-GPC (16:0/20:3n3 or 6) levels	26	0.0022	0.8147	0.7147	0.9287
GCST90200757	Glycine to alanine ratio	20	0.0027	0.8343	0.7413	0.9390
GCST90200907	Retinol (Vitamin A) to linoleoyl-arachidonoyl-glycerol (18:2 to 20:4) [1] ratio	24	0.0028	0.8132	0.7102	0.9313
GCST90199787	Homostachydrine levels	24	0.0028	0.7497	0.6206	0.9056
GCST90200410	Phytanate levels	22	0.0030	1.3046	1.0944	1.5552
GCST90200073	1-linoleoyl-2-arachidonoyl-GPC (18:2/20:4n6) levels	27	0.0034	1.1820	1.0570	1.3217
GCST90199819	Tryptophan betaine levels	34	0.0034	0.8294	0.7319	0.9400
GCST90200322	Beta-hydroxyisovalerate levels	28	0.0045	1.2312	1.0666	1.4213
GCST90199903	2-oxoarginine levels	21	0.0060	0.7617	0.6272	0.9250
GCST90200866	Phosphate to asparagine ratio	30	0.0061	0.8425	0.7454	0.9522
GCST90199959	O-sulfo-l-tyrosine levels	26	0.0063	0.7993	0.6806	0.9387
GCST90200277	Bilirubin degradation product, C16H18N2O5 (1) levels	23	0.0072	0.8759	0.7953	0.9647
GCST90200959	Choline phosphate to choline ratio	22	0.0073	0.7862	0.6595	0.9373
GCST90200983	Cholesterol to linoleoyl-arachidonoyl-glycerol (18:2 to 20:4) [1] ratio	22	0.0075	0.8556	0.7632	0.9591
GCST90200786	Cysteine to alanine ratio	28	0.0080	0.8033	0.6832	0.9445
GCST90200808	Spermidine to choline ratio	17	0.0080	1.3690	1.0852	1.7270
GCST90199904	Pantoate levels	27	0.0084	1.2549	1.0600	1.4857
GCST90200122	Nisinate (24:6n3) levels	18	0.0092	1.2229	1.0511	1.4228
GCST90200274	Cis-3,4-methyleneheptanoylglycine levels	24	0.0097	0.8477	0.7479	0.9608
GCST90200171	Perfluorooctanoate (PFOA) levels	22	0.0115	1.2857	1.0580	1.5625
GCST90200700	Decadienedioic acid (C10:2-DC) levels	22	0.0118	0.8956	0.8219	0.9759
GCST90200414	Myristate (14:0) levels	23	0.0125	1.2785	1.0544	1.5502
GCST90200186	8-methoxykynurenate levels	26	0.0132	0.7928	0.6597	0.9526
GCST90199705	Propionylglycine levels	21	0.0135	0.8555	0.7558	0.9683
GCST90199741	Gamma-glutamylglycine levels	27	0.0146	0.8574	0.7578	0.9700
GCST90200067	1-stearoyl-2-linoleoyl-GPI (18:0/18:2) levels	28	0.0155	0.8451	0.7374	0.9684
GCST90200992	Alanine to asparagine ratio	34	0.0165	0.8699	0.7763	0.9748
GCST90199820	Dihomo-linolenate (20:3n3 or n6) levels	24	0.0167	0.8066	0.6764	0.9618
GCST90201018	Bilirubin (Z,Z) to glucuronate ratio	21	0.0174	0.8610	0.7611	0.9740
GCST90199793	1-linoleoyl-GPE (18:2) levels	33	0.0180	0.8656	0.7681	0.9755
GCST90200535	X-17325 levels	24	0.0186	0.8331	0.7155	0.9700
GCST90200216	Sulfate of piperine metabolite C18H21NO3 (3) levels	23	0.0187	1.2425	1.0368	1.4891

(*Continued*)

Table 1 (Continued).

ID.exposure	Exposure	Nsnp	p-value	OR	OR_lci95	OR_uci95
GCST90199960	N-formylanthranilic acid levels	23	0.0198	0.8709	0.7753	0.9783
GCST90199688	N-acetylglycine levels	23	0.0199	0.8484	0.7388	0.9744
GCST90199886	3-methylglutaconate levels	21	0.0210	0.8758	0.7826	0.9802
GCST90200251	Branched-chain, straight-chain, or cyclopropyl 10:1 fatty acid (1) levels	17	0.0211	0.8744	0.7802	0.9800
GCST90199785	Isovalerylglycine levels	24	0.0225	0.8646	0.7630	0.9797
GCST90200452	Plasma free asparagine levels	26	0.0229	1.1626	1.0211	1.3237
GCST90199678	Tartronate (hydroxymalonate) levels	19	0.0234	0.8441	0.7290	0.9773
GCST90199933	3b-hydroxy-5-cholenoic acid levels	29	0.0239	1.1881	1.0231	1.3796
GCST90200308	3-hydroxyisobutyrate levels	19	0.0258	1.2604	1.0283	1.5448
GCST90200534	X-16580 levels	18	0.0271	1.2607	1.0266	1.5481
GCST90199921	Dihydroferulate levels	13	0.0274	0.7604	0.5961	0.9699
GCST90199996	Sphingomyelin (d18:1/20:1, d18:2/20:0) levels	27	0.0297	1.1792	1.0164	1.3682
GCST90200787	Glutamine to asparagine ratio	26	0.0297	0.8626	0.7550	0.9856
GCST90200472	X-11850 levels	22	0.0300	0.8200	0.6854	0.9809
GCST90200988	Benzoate to linoleoyl-arachidonoyl-glycerol (18:2 to 20:4) [1] ratio	16	0.0301	0.8310	0.7030	0.9823
GCST90199892	Isoursodeoxycholate levels	19	0.0304	1.2265	1.0195	1.4755
GCST90200748	Aspartate to glutamate ratio	25	0.0309	1.2262	1.0189	1.4756
GCST90200987	Benzoate to oleoyl-linoleoyl-glycerol (18:1 to 18:2) [2] ratio	31	0.0312	0.8512	0.7353	0.9855
GCST90200842	Citrate to oxalate (ethanedioate) ratio	16	0.0315	1.2625	1.0209	1.5613
GCST90200823	Adenosine 5′-diphosphate (ADP) to N-palmitoyl-sphingosine (d18:1 to 16:0) ratio	23	0.0327	1.1470	1.0113	1.3010
GCST90200362	Succinate levels	25	0.0332	1.0977	1.0075	1.1960
GCST90200174	3-hydroxybutyroylglycine levels	27	0.0355	0.8701	0.7642	0.9906
GCST90199706	Butyrylglycine levels	22	0.0359	0.9042	0.8231	0.9934
GCST90200278	3-hydroxyoctanoylcarnitine (2) levels	17	0.0368	1.2404	1.0133	1.5185
GCST90200621	X-23739 levels	27	0.0387	1.2141	1.0102	1.4593
GCST90199652	1-stearoyl-2-oleoyl-GPS (18:0/18:1) levels	20	0.0387	1.2887	1.0132	1.6391
GCST90200109	Linoleoyl-arachidonoyl-glycerol (18:2/20:4) [2] levels	33	0.0394	1.1296	1.0060	1.2685
GCST90200797	Spermidine to N-acetylputrescine ratio	21	0.0401	1.1611	1.0068	1.3391
GCST90200010	Sphingomyelin (d18:1/22:1, d18:2/22:0, d16:1/24:1) levels	22	0.0404	1.1991	1.0080	1.4264
GCST90200476	X-11843 levels	23	0.0414	0.8370	0.7055	0.9931
GCST90200760	Methionine to methionine sulfoxide ratio	27	0.0414	0.8357	0.7033	0.9930
GCST90200217	(2,4 or 2,5)-dimethylphenol sulfate levels	21	0.0427	1.2003	1.0060	1.4321
GCST90199640	4-guanidinobutanoate levels	19	0.0427	1.1334	1.0041	1.2793
GCST90200115	N-palmitoyl-heptadecasphingosine (d17:1/16:0) levels	28	0.0439	1.1542	1.0039	1.3270

(*Continued*)

Table 1 (Continued).

ID.exposure	Exposure	Nsnp	p-value	OR	OR_lci95	OR_uci95
GCST90200405	Retinol (Vitamin A) levels	28	0.0461	0.8408	0.7090	0.9970
GCST90200928	N-palmitoyl-sphingosine (d18:1 to 16:0) to N-stearoyl-sphingosine (d18:1 to 18:0) ratio	20	0.0468	0.8575	0.7369	0.9978
GCST90200692	1-palmitoyl-2-arachidonoyl-gpc (16:0/20:4n6) levels	31	0.0469	1.0902	1.0012	1.1871
GCST90200239	Tetradecadienedioate (C14:2-DC) levels	25	0.0471	0.8800	0.7756	0.9984
GCST90199880	Cis-4-decenoylcarnitine (C10:1) levels	27	0.0476	1.1279	1.0013	1.2704
GCST90200273	2-methoxyhydroquinone sulfate (2) levels	22	0.0485	0.8772	0.7701	0.9991
GCST90200923	Glycerol to mannitol to sorbitol ratio	26	0.0494	0.8362	0.6995	0.9995
GCST90199692	Citramalate levels	24	0.0495	0.8520	0.7262	0.9997
GCST90199935	Glycohyocholate levels	17	0.0496	1.2203	1.0003	1.4888

Table 2 The Causal Relationship Between 19 Significantly Correlated Circulating Metabolites and Pressure Ulcer Demonstrated by IVW Method for MR Analysis

ID.exposure	Exposure	Nsnp	p-value	OR	OR_lci95	OR_uci95
GCST90200808	Spermidine to choline ratio	17	0.0080	1.3690	1.0852	1.7270
GCST90200410	Phytanate levels	22	0.0030	1.3046	1.0944	1.5552
GCST90200058	1-(1-enyl-stearoyl)-2-arachidonoyl-GPE (p-18:0/20:4) levels	24	0.0005	1.3008	1.1228	1.5071
GCST90199904	Pantoate levels	27	0.0084	1.2549	1.0600	1.4857
GCST90200322	Beta-hydroxyisovalerate levels	28	0.0045	1.2312	1.0666	1.4213
GCST90200073	1-linoleoyl-2-arachidonoyl-GPC (18:2/20:4n6) levels	27	0.0034	1.1820	1.0570	1.3217
GCST90200103	Linoleoyl-arachidonoyl-glycerol (18:2/20:4) [1] levels	20	0.0016	1.1791	1.0646	1.3058
GCST90200277	Bilirubin degradation product, C16H18N2O5 (1) levels	23	0.0072	0.8759	0.7953	0.9647
GCST90200983	Cholesterol to linoleoyl-arachidonoyl-glycerol (18:2 to 20:4) [1] ratio	22	0.0075	0.8556	0.7632	0.9591
GCST90200866	Phosphate to asparagine ratio	30	0.0061	0.8425	0.7454	0.9522
GCST90200757	Glycine to alanine ratio	20	0.0027	0.8343	0.7413	0.9390
GCST90199819	Tryptophan betaine levels	34	0.0034	0.8294	0.7319	0.9400
GCST90200051	1-palmitoyl-2-dihomo-linolenoyl-GPC (16:0/20:3n3 or 6) levels	26	0.0022	0.8147	0.7147	0.9287
GCST90200907	Retinol (Vitamin A) to linoleoyl-arachidonoyl-glycerol (18:2 to 20:4) [1] ratio	24	0.0028	0.8132	0.7102	0.9313
GCST90200786	Cysteine to alanine ratio	28	0.0080	0.8033	0.6832	0.9445
GCST90199959	O-sulfo-l-tyrosine levels	26	0.0063	0.7993	0.6806	0.9387
GCST90200959	Choline phosphate to choline ratio	22	0.0073	0.7862	0.6595	0.9373
GCST90199903	2-oxoarginine levels	21	0.0060	0.7617	0.6272	0.9250
GCST90199787	Homostachydrine levels	24	0.0028	0.7497	0.6206	0.9056

https://doi.org/10.2147/JIR.S503370

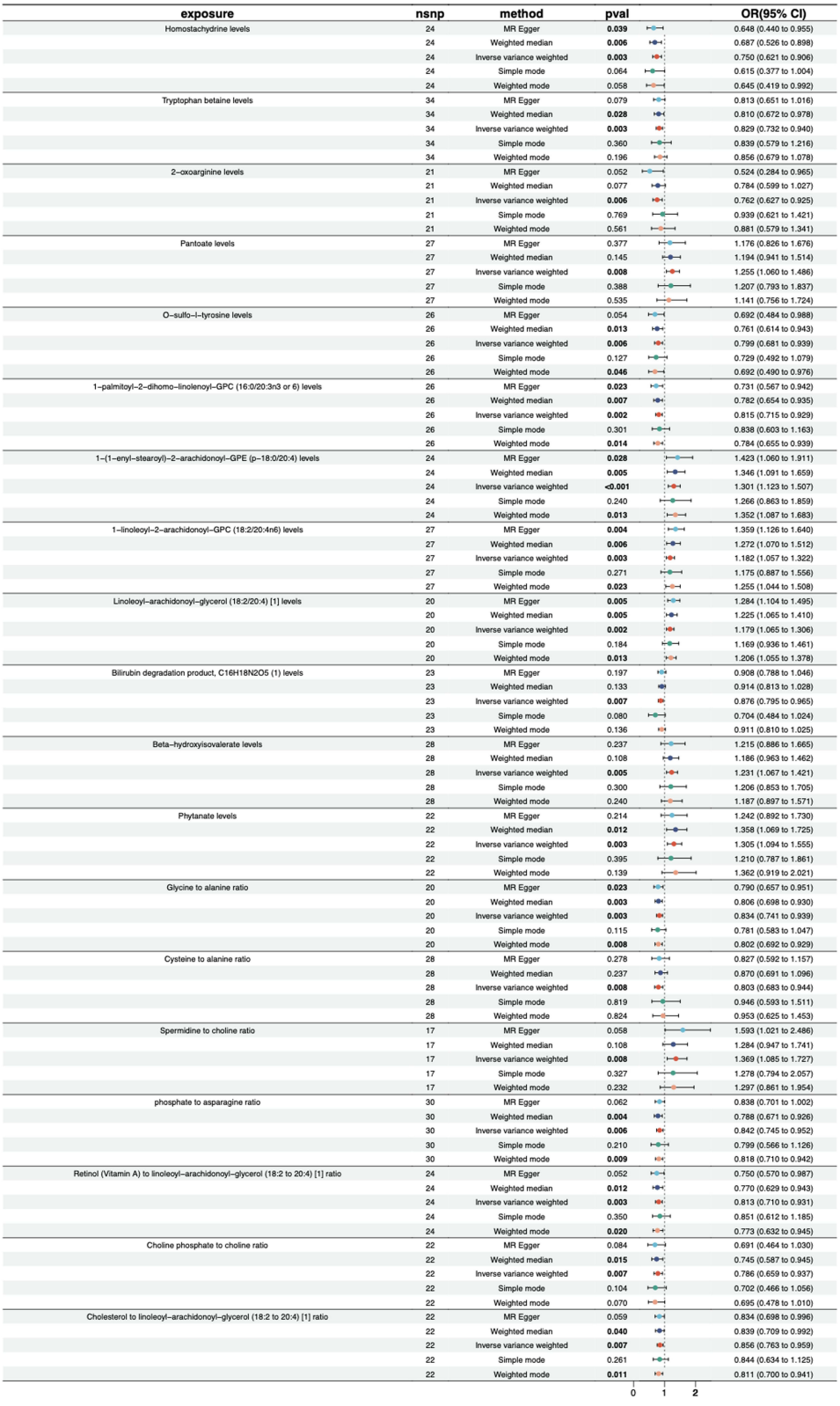

Figure 3 Forest plot illustrating the causal relationships between 19 significantly associated circulating metabolites and PU.

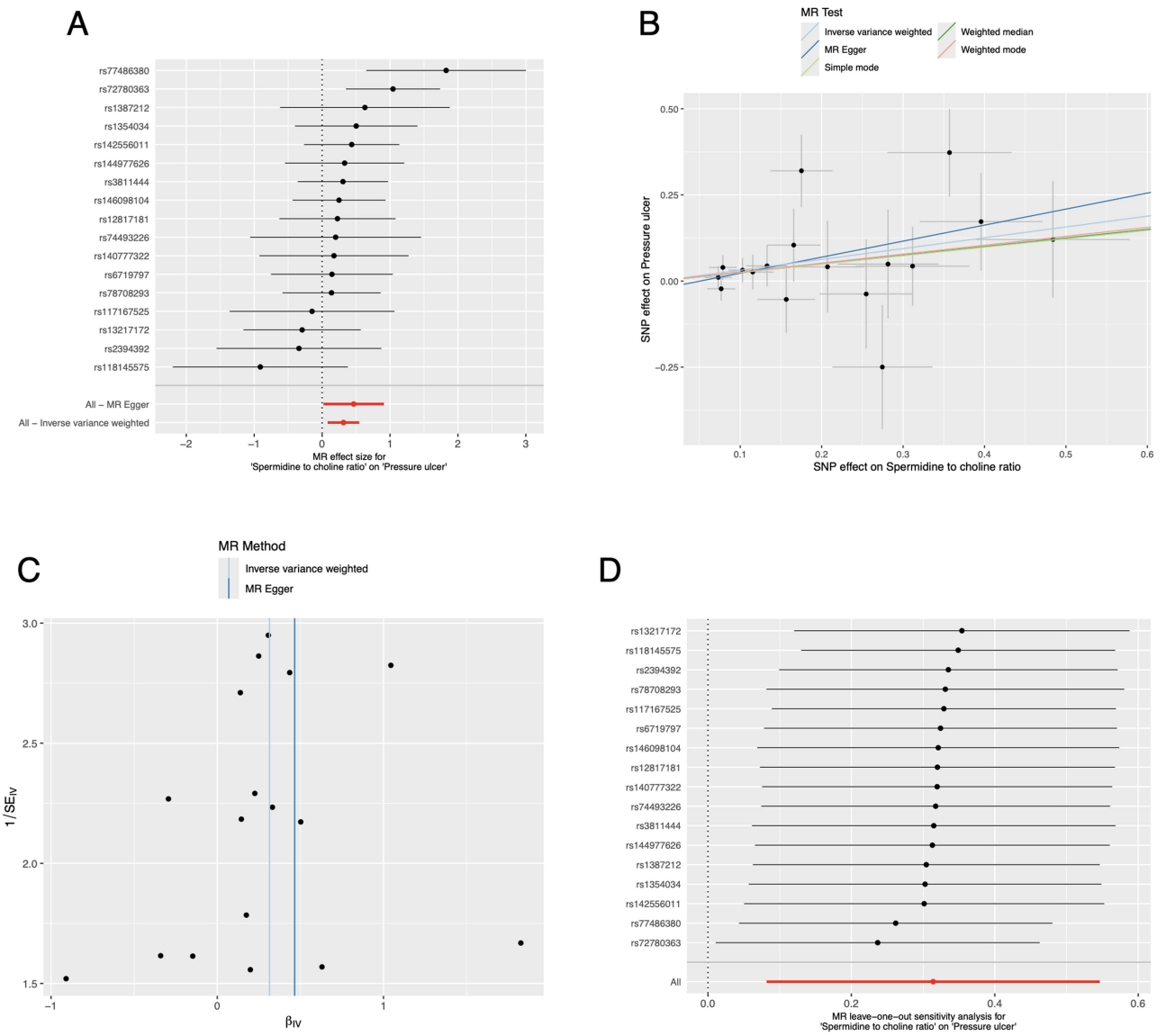

Figure 4 Causal analysis of the Spermidine to choline ratio on PU progression. (**A**) The forest plot illustrates the causal relationship of the spermidine to choline ratio with the progression of PU. (**B**) The scatter plot displays the causal impact of each SNP on PU progression. (**C**) The funnel plot indicates the overall heterogeneity of the MR estimates regarding the effect of the spermidine to choline ratio on PU progression. (**D**) The leave-one-out plot demonstrates the causal influence of the spermidine to choline ratio on PU progression when any single SNP is removed.

with eschar and exhibited significant inflammation, whereas the HD-Hom and HR (Spe/Cho) groups showed nearly complete recovery, with well-formed new epithelial tissue and minimal residual wound area ($P<0.001$). Although the LD-Hom group showed some improvement, its effects were less pronounced compared to the HD-Hom and HR (Spe/Cho) groups ($P<0.05$). In conclusion, Homostachydrine and HR (Spe/Cho) demonstrated significant potential in promoting wound healing in a rat model of PU.

https://doi.org/10.2147/JIR.S503370

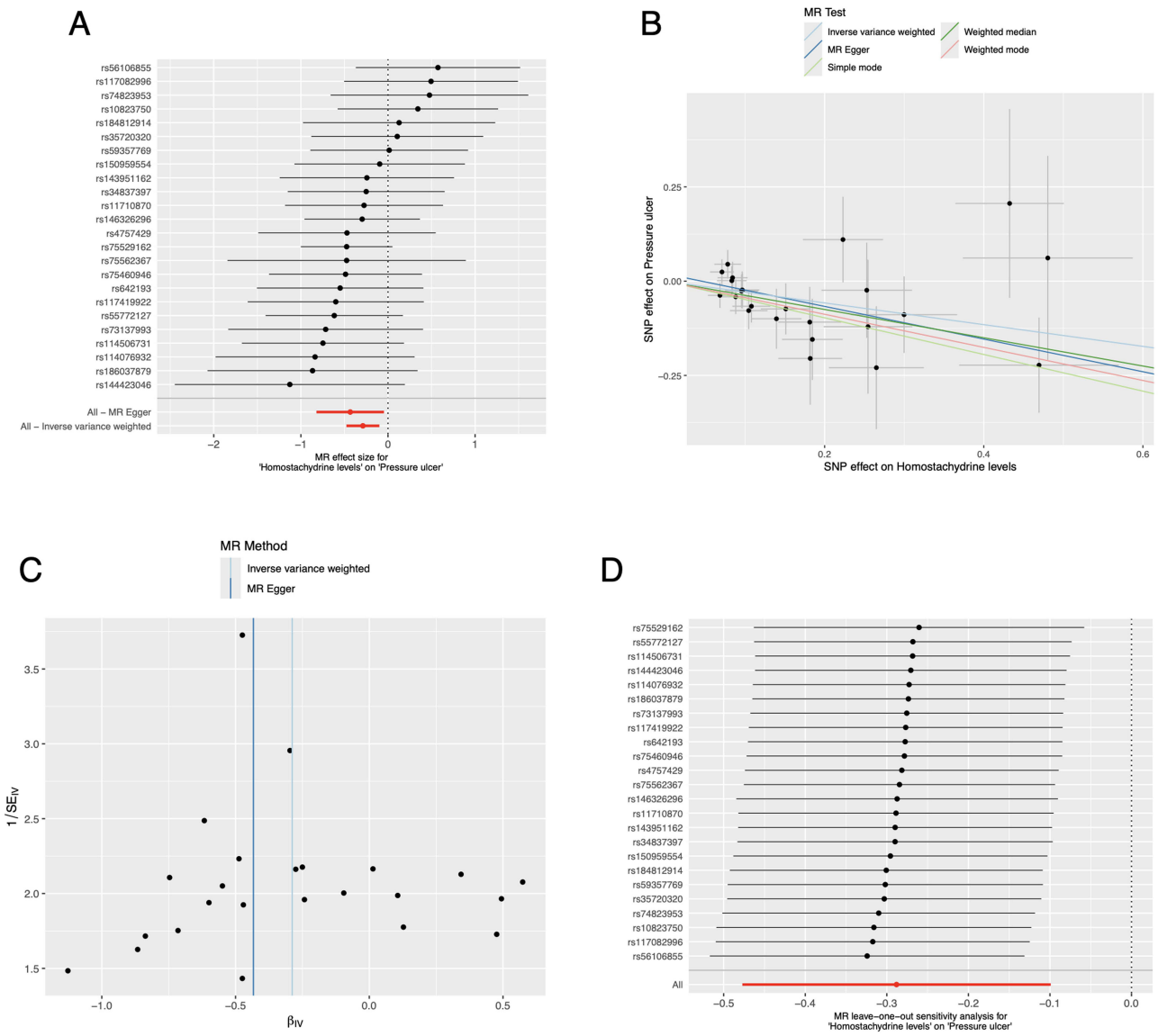

Figure 5 Causal analysis of the Homostachydrine levels on PU progression. (**A**) The forest plot illustrates the causal relationship of homostachydrine levels with the healing of PU. (**B**) The scatter plot displays the causal impact of each SNP on PU healing. (**C**) The funnel plot indicates the overall heterogeneity of the MR estimates regarding the effect of homostachydrine levels on PU healing. (**D**) The leave-one-out plot demonstrates the causal influence of homostachydrine levels on PU healing when any single SNP is removed.

Homostachydrine and HR (Spe/Cho) Reduce Skin Pathological Damage and Inflammatory Cell Infiltration, and Promote Collagen Deposition and Recombination on Pressure Sore Wounds

We evaluated the effects of Homostachydrine and Spermidine/choline on tissue repair in a rat model of PU using HE staining and Masson staining. On day 1 post-treatment, no significant differences were observed among the groups (Figure 7A and B). By day 3, HE staining revealed obvious inflammatory exudation and incomplete scab coverage in the model group, with the LR (Spe/Cho) group showing a similar pattern to the model group. In contrast, the LD-Hom group exhibited dry wounds with no exudation, thin scab formation, and a favorable healing trend, while the HD-Hom and HR (Spe/Cho) groups demonstrated even more significant improvements. Meanwhile, Masson staining showed fewer and unevenly distributed collagen fibers in the model and LR(Spe/Cho) groups, whereas the LD-Hom group began to display more organized collagen deposition, and the HD-Hom and HR(Spe/Cho) groups showed abundant collagen deposition

Table 3 The Causal Effect of Spermidine to Choline Ratio and Homostachydrine Levels on Pressure Ulcer Evaluated by IVW Method for MR Analysis

Method	Nsnp	B	SE	p-value	Low_ci	Up_ci	OR	OR_lci95	OR_uci95	Heterogeneity_Q_p-val	Pleiotropy_p-val	PRESSO_p-val
Spermidine to choline ratio												
MR Egger	17	0.4655	0.2270	0.0583	0.0205	0.9105	1.5928	1.0207	2.4856	0.2640		
Weighted median	17	0.2499	0.1555	0.1082	−0.0550	0.5547	1.2838	0.9465	1.7414			
Inverse variance weighted	17	0.3141	0.1185	0.0080	0.0818	0.5464	1.3690	1.0852	1.7270	0.2838	0.4445	0.3290
Simple mode	17	0.2455	0.2427	0.3269	−0.2302	0.7212	1.2782	0.7943	2.0568			
Weighted mode	17	0.2599	0.2091	0.2318	−0.1499	0.6697	1.2968	0.8608	1.9536			
Homostachydrine levels												
MR Egger	24	−0.4332	0.1976	0.0392	−0.8204	−0.0460	0.6484	0.4402	0.9551	0.7542		
Weighted median	24	−0.3750	0.1367	0.0061	−0.6430	−0.1071	0.6873	0.5257	0.8985			
Inverse variance weighted	24	−0.2881	0.0964	0.0028	−0.4771	−0.0991	0.7497	0.6206	0.9056	0.7643	0.4092	0.7840
Simple mode	24	−0.4860	0.2498	0.0640	−0.9756	0.0035	0.6151	0.3770	1.0035			
Weighted mode	24	−0.4389	0.2197	0.0577	−0.8695	−0.0082	0.6448	0.4192	0.9918			

https://doi.org/10.2147/JIR.S503370

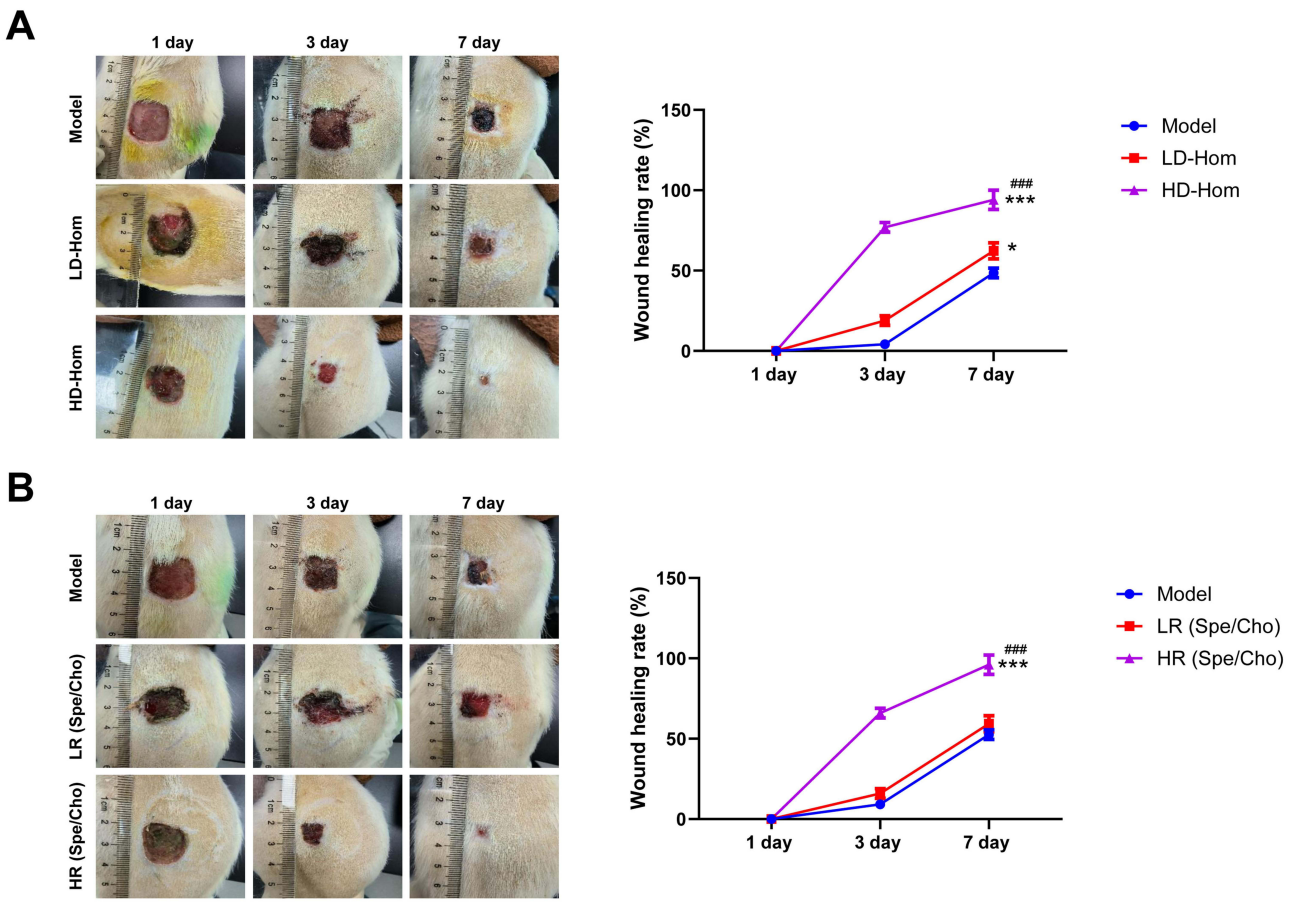

Figure 6 Homostachydrine and HR (Spe/Cho) promote the healing of pressure ulcer wounds. (**A**) Observation of wound healing on days 1, 3, and 7 under Homostachydrine treatment. (**B**) Evaluation of wound healing status on days 1, 3, and 7 after treatment with Spermidine/Choline. *$p < 0.05$, ***$p < 0.001$ vs Model, ### $p< 0.001$ vs LD-Hom or LR (Spe/Cho).

with well-arranged structures (Figure 7A and B). By day 7, the HD-Hom and HR (Spe/Cho) groups exhibited intact epidermis with only slight thickening and reduced numbers of hair follicles and sebaceous glands in the dermis, with no other significant abnormalities observed in HE staining. In Masson staining, these groups showed abundant collagen deposition with a loose arrangement. In contrast, the model and LR (Spe/Cho) groups displayed extensive skin damage, including thickened and ruptured epidermis partially separated from the dermis, lack of collagen, hair follicles, sebaceous glands, and subcutaneous fat at the wound site, along with significant granulation tissue formation and inflammatory cell infiltration in HE staining. In Masson staining, the model and LR (Spe/Cho) groups showed sparse collagen with weak and uneven staining. The LD-Hom group demonstrated some improvement but was less effective than the HD-Hom and HR(Spe/Cho) groups (Figure 7A and B). In conclusion, Homostachydrine and HR (Spe/Cho) not only significantly reduced skin pathological damage and inflammatory cell infiltration but also promoted collagen deposition and reorganization, thereby accelerating wound healing.

Homostachydrine and HR (Spe/Cho) Promote the Expression of Proteins Associated with Pressure Sore Wound Healing and Inhibit the Expression of Inflammatory Factors

Finally, we employed Western blot analysis to investigate the effects of Homostachydrine and Spermidine/choline on the expression levels of the inflammatory factor TNF-α and wound healing-related proteins (Col-I and Col-III). The results revealed that, compared to the Model group, both LD-Hom and LR (Spe/Cho) significantly decreased the levels of the inflammatory factor TNF-α. Additionally, these treatments effectively promoted the expression of Col-I and Col-III (P<0.01, P<0.001, Figure 8A and B). Furthermore, compared to LD-Hom and LR (Spe/Cho) respectively, HD-Hom and

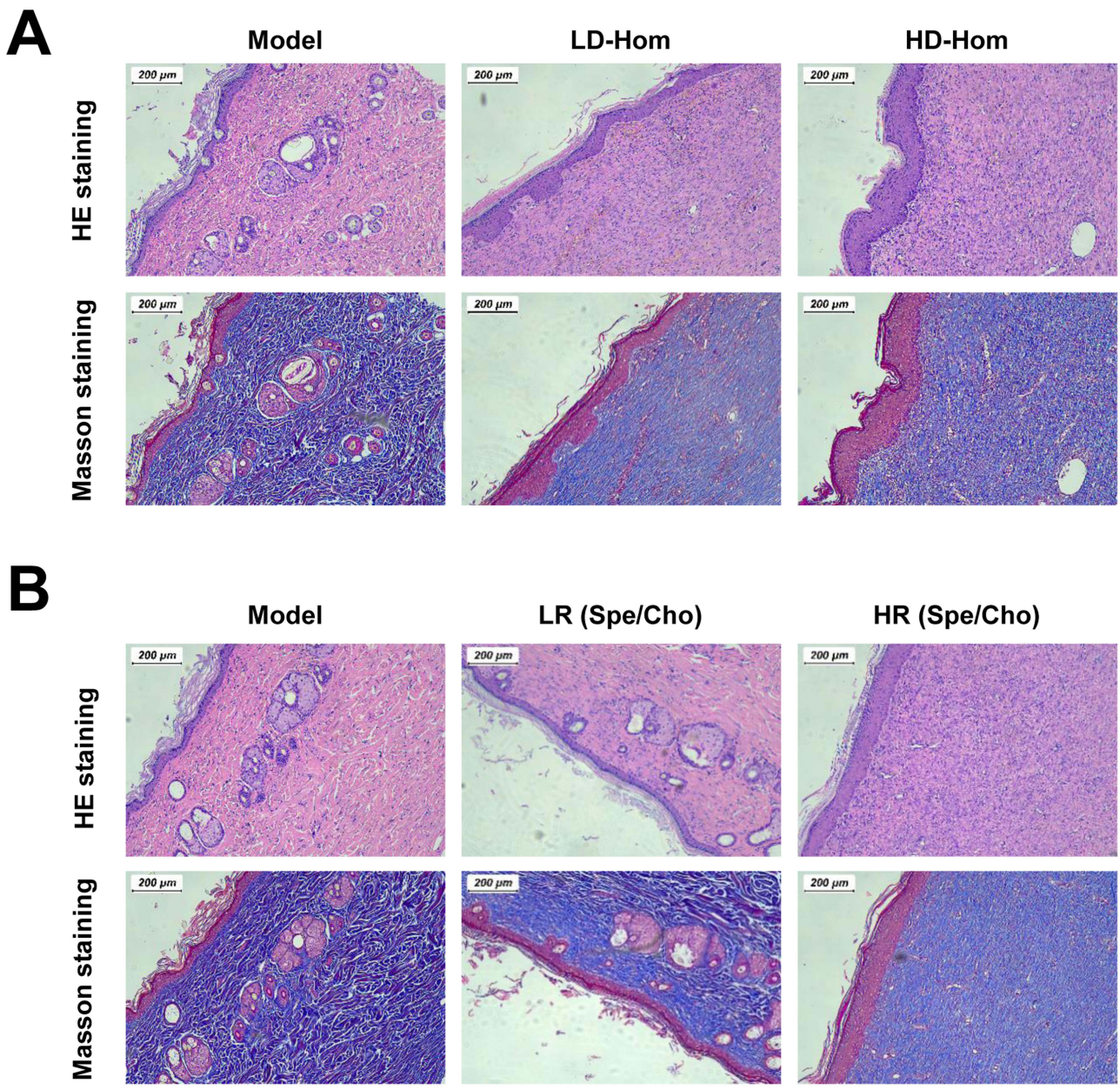

Figure 7 Homostachydrine and HR (Spe/Cho) reduce skin pathological damage and inflammatory cell infiltration, and promote collagen deposition and recombination on pressure sore wounds. (**A**) Histological analysis of wound healing by HE staining and Masson staining was treated with Homostachydrine treatment. (**B**) Wound healing was histologically analyzed through HE staining and Masson staining after Spermidine/Choline treatment.

HR (Spe/Cho) demonstrated an even stronger ability to reduce TNF-α levels, and enhance the expression of Col-I and Col-III ($P<0.01$, $P<0.001$, Figure 8A and B). This suggests that Homostachydrine and HR (Spe/Cho) not only modulate the expression of proteins associated with wound healing but also significantly suppress inflammatory responses, thereby accelerating the wound repair process.

Discussion

The development of PU is influenced by factors such as impaired tissue perfusion, patient positioning, nutrition, hydration, and vasoactive medications.[32] Although the relationship between circulating metabolites in PU has also been mentioned in studies, its association with PU remains unclear. In this study, we used a two-sample MR approach to explore the causal relationship between 1400 circulating metabolites and pressure ulcer (PU) risk. Our findings revealed

https://doi.org/10.2147/JIR.S503370

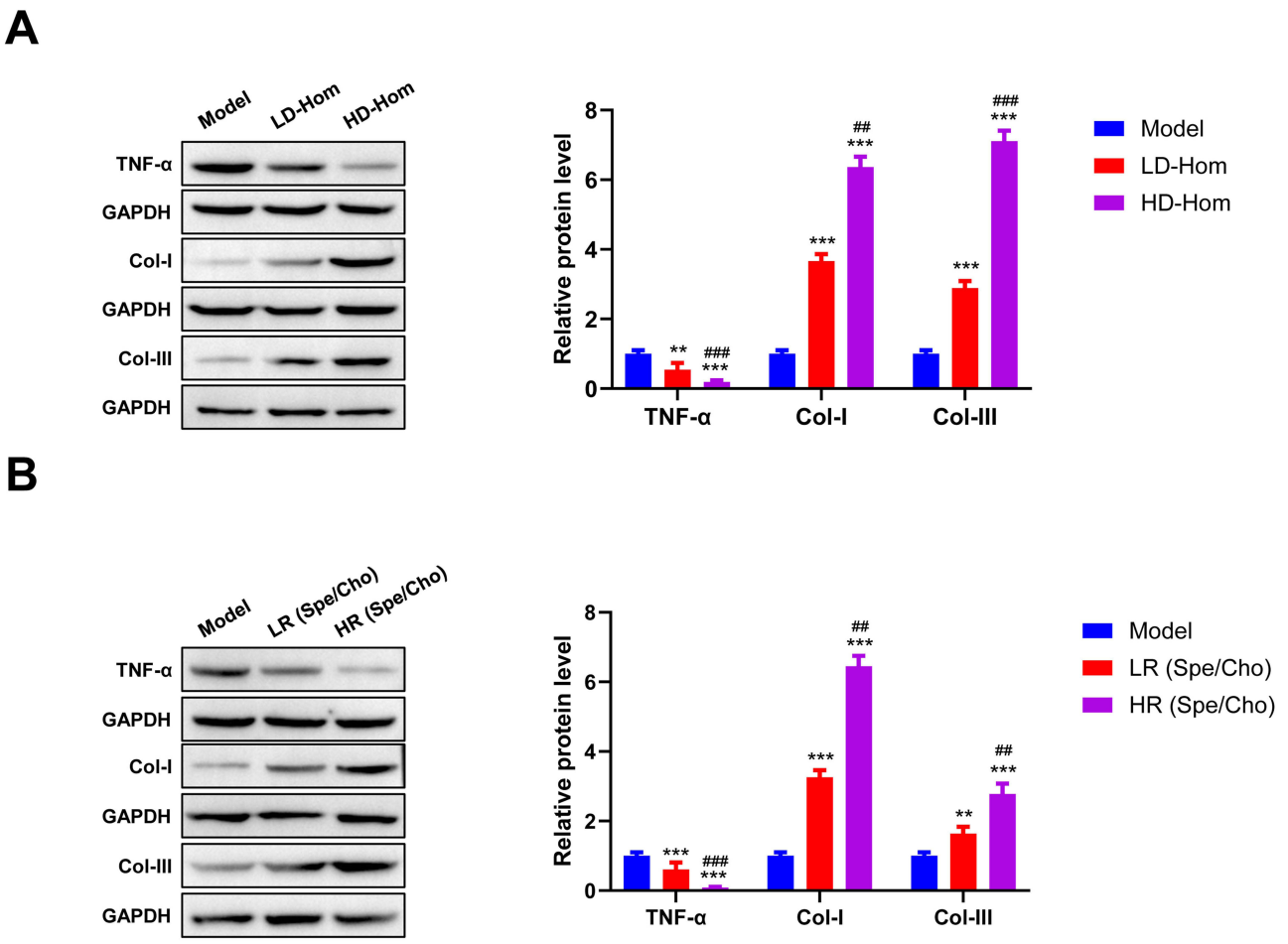

Figure 8 Homostachydrine and HR (Spe/Cho) promote the expression of proteins associated with pressure sore wound healing and inhibit the expression of inflammatory factors. (**A**) Western blot analysis of protein levels (TNF-α levels, Col-I, and Col-III) in response to Homostachydrine treatment. (**B**) The protein levels of TNF-α, Col-I, and Col-III were assessed using Western blot analysis after treatment with Spermidine/Choline. $^{**}p < 0.01$, $^{***}p < 0.001$ vs Model, $^{\#\#}p < 0.01$, $^{\#\#\#}p < 0.001$ vs LD-Hom or LR (Spe/Cho).

that 19 metabolites had significant causal effects with PU, emphasizing the potential role of metabolic pathways in understanding the mechanisms of PU occurrence. This study successfully identified at the SNP level that Spermidine to choline ratio and Homostachydrine levels have a significant impact on PU. These results not only extend our understanding of PU risk factors, but also suggest the potential benefits of metabolism-targeted interventions that can be used in PU prevention strategies.

Metabolites are small molecules that are intermediates or end products of metabolic reactions. Their levels are influenced by a variety of factors, including genetics, diet and lifestyle, gut flora, and disease.[33,34] They may also influence disease risk and are targets for therapeutic interventions.[35] Understanding the causal role of metabolites in the etiology of disease can provide readily addressable points of intervention for treatment. One way to assess the role of metabolites in disease outcomes is through human genetics. In our investigation, we identified 19 plasma metabolites that demonstrated significant associations with PUs. Among them, 7 metabolites were linked to PU increased risk. The spermidine to choline ratio emerged as a crucial indicator, as choline serves as an essential component of cell membranes and maintains membrane integrity, while spermidine exhibits antioxidant and anti-inflammatory properties.[36] Disruption of this ratio may compromise cell membrane stability and tissue repair capabilities.[37] Therefore, the increased spermidine/choline ratio may elevate the risk of PU through mechanisms such as impaired cell membrane stability, enhanced chronic inflammation, dysregulated autophagy, and impaired neurovascular regulation, leading to cells being more susceptible to stress damage, impaired tissue repair, and microcirculatory dysfunction. Phytanate, a fatty acid metabolite,

was found to be potentially linked to tissue inflammatory responses and oxidative stress, with abnormal levels possibly affecting local tissue metabolism and healing processes.[18] The compound 1-(1-enyl-stearoyl)-2-arachidonoyl-GPE (p-18:0/20:4), a major constituent of cell membranes, participates in cell signaling pathways and may influence membrane integrity and repair mechanisms during pressure-induced injury.[38] Pantoate, a vitamin B5 precursor, plays a vital role in energy metabolism and lipid synthesis, potentially affecting local tissue energy supply and repair capacity.[39,40] Beta-hydroxyisovalerate, an intermediate metabolite of branched-chain amino acid metabolism, may reflect local tissue metabolic status, with its fluctuations potentially correlating with tissue injury repair processes.[41] Both 1-linoleoyl-2-arachidonoyl-GPC (18:2/20:4n6) and Linoleoyl-arachidonoyl-glycerol (18:2/20:4) are involved in inflammatory responses and cell signaling cascades, potentially modulating the inflammatory processes in PUs and contributing to tissue repair and regeneration.[42–44] These metabolites demonstrate potential clinical applications as biomarkers for PU risk assessment, progression monitoring, and treatment evaluation, thereby offering promising tools for early warning systems and therapeutic outcome assessment in PU management.

Our study identified 12 metabolites that demonstrate protective effects against pressure ulcer (PU) development. Bilirubin degradation product exhibits antioxidant properties, mitigates tissue inflammation, and protects cells from oxidative stress damage.[45,46] The ratio of cholesterol to linoleoyl-arachidonoyl-glycerol (18:2 to 20:4) reflects cell membrane fluidity and stability, influencing tissue pressure tolerance and cellular repair capacity.[47] The phosphate to asparagine ratio and glycine to alanine ratio both impact energy metabolism and protein synthesis, participating in cell signaling pathways and potentially affecting tissue repair rates.[48,49] Tryptophan betaine demonstrates anti-inflammatory properties, modulates stress responses, and may enhance tissue tolerance. The 1-palmitoyl-2-dihomo-linolenoyl-GPC (16:0/20:3n3 or 6) maintains cell membrane integrity, participates in cell signaling, and influences tissue repair processes.[50] The ratio of retinol (Vitamin A) to linoleoyl-arachidonoyl-glycerol promotes epithelial cell renewal, enhances immune function, and accelerates wound healing.[51] The cysteine to alanine ratio participates in antioxidant processes, affects collagen cross-linking, and strengthens tissue integrity.[52] O-sulfo-l-tyrosine is involved in protein modification and cell signaling pathways, potentially contributing to tissue repair.[53] The choline phosphate to choline ratio reflects cell membrane metabolic status, influences neural conduction, and relates to tissue nutrient supply.[54] 2-oxoarginine participates in nitric oxide metabolism, affects vascular function, and may improve local blood supply.[55] And Homostachydrine levels, which demonstrate anti-inflammatory effects, improve microcirculation, and enhance tissue tolerance.[56,57]

It is worth noting that our animal experiments further validated the role of these metabolites in the development and repair of PU. In the PU rat model, animals exhibited more severe skin damage, slower wound healing rates, and higher levels of chronic inflammation. Furthermore, rats supplemented with homostachydrine and a high ratio of Spermidine/Choline showed faster wound closure and lower levels of inflammation, further supporting its potential value in PU prevention and treatment. These animal experiment results not only confirmed the causal relationship between metabolites and PU risk but also provided experimental evidence for metabolic interventions.

The identification of specific circulating metabolites associated with PU risk opens avenues for clinical applications. Metabolic profiling could potentially serve as a predictive tool for PU risk assessment, enabling clinicians to implement preventive measures in high-risk populations. Additionally, the therapeutic modulation of these metabolites could be investigated as a novel strategy for PU management. For instance, since an elevated spermidine-to-choline ratio is linked to increased PU risk, modulating its levels could be a viable preventive or therapeutic strategy. For example, supplementing choline or reducing spermidine intake may help stabilize cell membrane integrity, thereby lowering PU susceptibility. Homostachydrine, identified as a protective factor against PU, suggests a potential therapeutic role. Exogenous supplementation or endogenous upregulation (via dietary modifications or metabolic enhancers) could increase its levels, thereby improving tissue resilience and promoting wound healing. These findings open avenues for future research into metabolism-targeted therapies, such as small-molecule drugs or functional nutrition interventions, aimed at optimizing metabolic profiles in PU patients to reduce ulcer incidence and accelerate healing. This study provides novel insights into PU-related metabolic biomarkers, paving the way for further investigations integrating multi-omics approaches to explore interactions between metabolites and other biological processes, ultimately improving PU diagnosis and personalized treatment.

While our study provides valuable insights into the causal relationships between circulating metabolites and PU, several limitations should be acknowledged. First, while our two-sample MR approach provides robust evidence for causal

relationships, the genetic variants were primarily derived from Finnish populations, potentially limiting generalizability across different ethnic groups. To enhance the applicability of our findings, future studies should incorporate multi-ethnic GWAS datasets to assess whether the identified metabolite-PU associations hold across different ancestries. Second, although we employed multiple sensitivity analyses, the inherent assumptions of MR studies and potential horizontal pleiotropy cannot be completely excluded. Third, the cross-sectional nature of GWAS data prevents detailed temporal analysis of metabolic changes. Finally, while our findings identify significant metabolite associations, the complex interactions between metabolites and environmental factors require further investigation through prospective clinical studies to fully elucidate their therapeutic potential in PU prevention and management.

Conclusions

This study highlights the significant causal relationships between circulating metabolites and the risk of PUs. The identified metabolites, particularly the spermidine to choline ratio and homostachydrine levels, offer promising targets for future research and clinical intervention. By enhancing our understanding of the metabolic underpinnings of PU, we can contribute to more effective prevention and treatment strategies, ultimately improving patient outcomes in this challenging area of healthcare.

Author Contributions

All authors made a significant contribution to the work reported, whether that is in the conception, study design, execution, acquisition of data, analysis and interpretation, or in all these areas; took part in drafting, revising or critically reviewing the article; gave final approval of the version to be published; have agreed on the journal to which the article has been submitted; and agree to be accountable for all aspects of the work.

Funding

This study was supported by Luzhou Science and Technology Plan (2023SYF123); the Doctoral Research Initiation Fund of Affiliated Hospital of Southwest Medical University.

Disclosure

The authors declare no conflicts of interest in this work.

References

1. Lustig A, Margi R, Orlov A, Orlova D, Azaria L, Gefen A. The mechanobiology theory of the development of medical device-related pressure ulcers revealed through a cell-scale computational modeling framework. *Biomech Model Mechanobiol*. 2021;20(3):851–860. doi:10.1007/s10237-021-01432-w
2. Torsy T, Serraes B, Beeckman D. Pressure ulcer risk assessment in the ICU: the importance of balancing systemic and body-site specific risk factors. *Intensive Crit Care Nurs*. 2024;86:103857. doi:10.1016/j.iccn.2024.103857
3. Lahmann NA, Kottner J. Relation between pressure, friction and pressure ulcer categories: a secondary data analysis of hospital patients using CHAID methods. *Int J Nurs Stud*. 2011;48(12):1487–1494. doi:10.1016/j.ijnurstu.2011.07.004
4. Okamoto S, Ogai K, Mukai K, Sugama J. Association of skin microbiome with the onset and recurrence of pressure injury in bedridden elderly people. *Microorganisms*. 2021;9(8). doi:10.3390/microorganisms9081603
5. Sayan HE, Girgin NK, Asan A. Prevalence of pressure ulcers in hospitalized adult patients in Bursa, Turkey: a multicentre, point prevalence study. *J Eval Clin Pract*. 2020;26(6):1669–1676. doi:10.1111/jep.13354
6. Cortés OL, Herrera-Galindo M, Villar JC, Rojas YA, Del Pilar Paipa M, Salazar L. Frequency of repositioning for preventing pressure ulcers in patients hospitalized in ICU: protocol of a cluster randomized controlled trial. *BMC Nurs*. 2021;20(1):121. doi:10.1186/s12912-021-00616-0
7. Sen D, McNeill J, Mendelson Y, Dunn R, Hickle K. A new vision for preventing pressure ulcers: wearable wireless devices could help solve a common-and serious-problem. *IEEE Pulse*. 2018;9(6):28–31. doi:10.1109/mpul.2018.2869339
8. Deprez JF, Brusseau E, Fromageau J, Cloutier G, Basset O. On the potential of ultrasound elastography for pressure ulcer early detection. *Med Phys*. 2011;38(4):1943–1950. doi:10.1118/1.3560421
9. Tavares C, Domingues MF, Paixão T, Alberto N, Silva H, Antunes P. Wheelchair pressure ulcer prevention using FBG based sensing devices. *Sensors*. 2019;20(1). doi:10.3390/s20010212
10. Guillén-Solà M, Soler Mieras A, Tomàs-Vidal AM. A multi-center, randomized, clinical trial comparing adhesive polyurethane foam dressing and adhesive hydrocolloid dressing in patients with grade II pressure ulcers in primary care and nursing homes. *BMC Fam Pract*. 2013;14:196. doi:10.1186/1471-2296-14-196
11. Niemiec SM, Louiselle AE, Liechty KW, Zgheib C. Role of microRNAs in pressure ulcer immune response, pathogenesis, and treatment. *Int J Mol Sci*. 2020;22(1). doi:10.3390/ijms22010064

12. Liao F, Burns S, Jan YK. Skin blood flow dynamics and its role in pressure ulcers. *J Tissue Viability*. 2013;22(2):25–36. doi:10.1016/j.jtv.2013.03.001
13. Niu D. Effect of Ma Yinglong Shexiang hemorrhoids cream combined with pearl powder on the pain and complications of severe pressure ulcer patients. *Medicine*. 2021;100(33):e26767. doi:10.1097/md.0000000000026767
14. Jin S, Newton MAA, Cheng H, et al. Progress of hydrogel dressings with wound monitoring and treatment functions. *Gels*. 2023;9(9). doi:10.3390/gels9090694
15. Hotamisligil GS. Inflammation, metaflammation and immunometabolic disorders. *Nature*. 2017;542(7640):177–185. doi:10.1038/nature21363
16. Brestoff JR, Artis D. Immune regulation of metabolic homeostasis in health and disease. *Cell*. 2015;161(1):146–160. doi:10.1016/j.cell.2015.02.022
17. Karin M, Clevers H. Reparative inflammation takes charge of tissue regeneration. *Nature*. 2016;529(7586):307–315. doi:10.1038/nature17039
18. Caliceti C, Rizzo P, Giuliano M. Role of natural compounds in oxidative stress and inflammation linked to cardiometabolic disorders: from biochemical aspects to clinical evidences. *Oxid Med Cell Longev*. 2018;2018:1479309. doi:10.1155/2018/1479309
19. Teckchandani S, Nagana Gowda GA, Raftery D, Curatolo M. Metabolomics in chronic pain research. *Eur J Pain*. 2021;25(2):313–326. doi:10.1002/ejp.1677
20. Birney E. Mendelian Randomization. *Cold Spring Harb Perspect Med*. 2022;12(4). doi:10.1101/cshperspect.a041302
21. Burgess S, Thompson SG. Interpreting findings from Mendelian randomization using the MR-Egger method. *Eur J Epidemiol*. 2017;32(5):377–389. doi:10.1007/s10654-017-0255-x
22. Georgakis MK, Gill D. Mendelian randomization studies in stroke: exploration of risk factors and drug targets with human genetic data. *Stroke*. 2021;52(9):2992–3003. doi:10.1161/strokeaha.120.032617
23. Ho J, Mak CCH, Sharma V, To K, Khan W. Mendelian randomization studies of lifestyle-related risk factors for osteoarthritis: a PRISMA review and meta-analysis. *Int J Mol Sci*. 2022;23(19). doi:10.3390/ijms231911906
24. Larsson SC, Butterworth AS, Burgess S. Mendelian randomization for cardiovascular diseases: principles and applications. *Eur Heart J*. 2023;44(47):4913–4924. doi:10.1093/eurheartj/ehad736
25. Sekula P, Del Greco MF, Pattaro C, Köttgen A. Mendelian randomization as an approach to assess causality using observational data. *J Am Soc Nephrol*. 2016;27(11):3253–3265. doi:10.1681/asn.2016010098
26. Raychaudhuri S. Mapping rare and common causal alleles for complex human diseases. *Cell*. 2011;147(1):57–69. doi:10.1016/j.cell.2011.09.011
27. Almasy L. The role of phenotype in gene discovery in the whole genome sequencing era. *Hum Genet*. 2012;131(10):1533–1540. doi:10.1007/s00439-012-1191-1
28. Zhang Q. Associating rare genetic variants with human diseases. *Front Genet*. 2015;6:133. doi:10.3389/fgene.2015.00133
29. Bucur IG, Claassen T, Heskes T. Inferring the direction of a causal link and estimating its effect via a Bayesian Mendelian randomization approach. *Stat Methods Med Res*. 2020;29(4):1081–1111. doi:10.1177/0962280219851817
30. Stadler I, Zhang RY, Oskoui P, Whittaker MS, Lanzafame RJ. Development of a simple, noninvasive, clinically relevant model of pressure ulcers in the mouse. *J Invest Surg*. 2004;17(4):221–227. doi:10.1080/08941930490472046
31. Sekiguchi A, Motegi SI, Uchiyama A, et al. Botulinum toxin B suppresses the pressure ulcer formation in cutaneous ischemia-reperfusion injury mouse model: possible regulation of oxidative and endoplasmic reticulum stress. *J Dermatol Sci*. 2018;90(2):144–153. doi:10.1016/j.jdermsci.2018.01.006
32. Lima Serrano M, González Méndez MI, Carrasco Cebollero FM, Lima Rodríguez JS. Factores de riesgo asociados al desarrollo de úlceras por presión en unidades de cuidados intensivos de adultos: revisión sistemática [Risk factors for pressure ulcer development in Intensive Care Units: a systematic review]. *Med Intensiva*. 2017;41(6):339–346. doi:10.1016/j.medin.2016.09.003
33. Chen Y, Lu T, Pettersson-Kymmer U, et al. Genomic atlas of the plasma metabolome prioritizes metabolites implicated in human diseases. *Nat Genet*. 2023;55(1):44–53. doi:10.1038/s41588-022-01270-1
34. Lee W-J, Hase K. Gut microbiota–generated metabolites in animal health and disease. *Nat Chem Biol*. 2014;2014:416–424. doi:10.1038/nchembio.1535
35. Wishart DS. Emerging applications of metabolomics in drug discovery and precision medicine. *Nat Rev Drug Discov*. 2016;2016:473–484. doi:10.1038/nrd.2016.32
36. Snider SA, Margison KD, Ghorbani P, et al. Choline transport links macrophage phospholipid metabolism and inflammation. *J Biol Chem*. 2018;293(29):11600–11611. doi:10.1074/jbc.RA118.003180
37. Merta H, Bahmanyar S. The inner nuclear membrane takes on lipid metabolism. *Dev Cell*. 2018;47(4):397–399. doi:10.1016/j.devcel.2018.11.005
38. Hishikawa D, Valentine WJ, Iizuka-Hishikawa Y, Shindou H, Shimizu T. Metabolism and functions of docosahexaenoic acid-containing membrane glycerophospholipids. *FEBS Lett*. 2017;591(18):2730–2744. doi:10.1002/1873-3468.12825
39. Dibble CC, Barritt SA, Perry GE, et al. PI3K drives the de novo synthesis of coenzyme A from vitamin B5. *Nature*. 2022;608(7921):192–198. doi:10.1038/s41586-022-04984-8
40. Gheita AA, Gheita TA, Kenawy SA. The potential role of B5: a stitch in time and switch in cytokine. *Phytother Res*. 2020;34(2):306–314. doi:10.1002/ptr.6537
41. Biswas D, Duffley L, Pulinilkunnil T. Role of branched-chain amino acid-catabolizing enzymes in intertissue signaling, metabolic remodeling, and energy homeostasis. *FASEB J*. 2019;33(8):8711–8731. doi:10.1096/fj.201802842RR
42. Calder PC. Mechanisms of action of (n-3) fatty acids. *J Nutr*. 2012;142(3):592s–599s. doi:10.3945/jn.111.155259
43. Sergeant S, Rahbar E, Chilton FH. Gamma-linolenic acid, Dihommo-gamma linolenic, Eicosanoids and Inflammatory Processes. *Eur J Pharmacol*. 2016;785:77–86. doi:10.1016/j.ejphar.2016.04.020
44. Brkić L, Riederer M, Graier WF, Malli R, Frank S. Acyl chain-dependent effect of lysophosphatidylcholine on cyclooxygenase (COX)-2 expression in endothelial cells. *Atherosclerosis*. 2012;224(2):348–354. doi:10.1016/j.atherosclerosis.2012.07.038
45. Nishizawa M, Hara T, Miura T, et al. Supplementation with a flavanol-rich lychee fruit extract influences the inflammatory status of young athletes. *Phytother Res*. 2011;25(10):1486–1493. doi:10.1002/ptr.3430
46. Ciftci O, Turkmen NB, Taslıdere A. Curcumin protects heart tissue against irinotecan-induced damage in terms of cytokine level alterations, oxidative stress, and histological damage in rats. *Naunyn Schmiedebergs Arch Pharmacol*. 2018;391(8):783–791. doi:10.1007/s00210-018-1495-3
47. Adebayo OL, Salau BA, Sandhir R, Adenuga GA. Dietary selenium or zinc supplementation restores brain lipid composition and membrane fluidity in protein-undernourished rats. *Dev Neurosci*. 2016;38(6):397–406. doi:10.1159/000462971

48. Carroll B, Korolchuk VI, Sarkar S. Amino acids and autophagy: cross-talk and co-operation to control cellular homeostasis. *Amino Acids*. 2015;47(10):2065–2088. doi:10.1007/s00726-014-1775-2
49. Pan S, Fan M, Liu Z, Li X, Wang H. Serine, glycine and one-carbon metabolism in cancer (Review). *Int J Oncol*. 2021;58(2):158–170. doi:10.3892/ijo.2020.5158
50. Li Q, You Y, Zeng Y, et al. Associations between plasma tryptophan and indole-3-propionic acid levels and mortality in patients with coronary artery disease. *Am J Clin Nutr*. 2022;116(4):1070–1077. doi:10.1093/ajcn/nqac170
51. Palmieri B, Vadalà M, Laurino C. Nutrition in wound healing: investigation of the molecular mechanisms, a narrative review. *J Wound Care*. 2019;28(10):683–693. doi:10.12968/jowc.2019.28.10.683
52. Perła-Kajan J, Utyro O, Rusek M, Malinowska A, Sitkiewicz E, Jakubowski H. N-Homocysteinylation impairs collagen cross-linking in cystathionine β-synthase-deficient mice: a novel mechanism of connective tissue abnormalities. *FASEB J*. 2016;30(11):3810–3821. doi:10.1096/fj.201600539
53. Hartmann-Fatu C, Trusch F, Moll CN, et al. Heterodimers of tyrosylprotein sulfotransferases suggest existence of a higher organization level of transferases in the membrane of the trans-Golgi apparatus. *J Mol Biol*. 2015;427(6 Pt B):1404–1412. doi:10.1016/j.jmb.2015.01.021
54. Obeid R, Awwad HM, Rabagny Y, Graeber S, Herrmann W, Geisel J. Plasma trimethylamine N-oxide concentration is associated with choline, phospholipids, and methyl metabolism. *Am J Clin Nutr*. 2016;103(3):703–711. doi:10.3945/ajcn.115.121269
55. Hannemann J, Böger R. Dysregulation of the nitric oxide/dimethylarginine pathway in hypoxic pulmonary vasoconstriction-molecular mechanisms and clinical significance. *Front Med*. 2022;9:835481. doi:10.3389/fmed.2022.835481
56. Moghadam SE, Moridi Farimani M, Soroury S, Ebrahimi SN, Jabbarzadeh E. Hypermongone C accelerates wound healing through the modulation of inflammatory factors and promotion of fibroblast migration. *Molecules*. 2019;24(10). doi:10.3390/molecules24102022
57. Parhiz H, Roohbakhsh A, Soltani F, Rezaee R, Iranshahi M. Antioxidant and anti-inflammatory properties of the citrus flavonoids hesperidin and hesperetin: an updated review of their molecular mechanisms and experimental models. *Phytother Res*. 2015;29(3):323–331. doi:10.1002/ptr.5256